

Assessment of DNA methylation differences between carriers of *APOE* ϵ 4 and *APOE* ϵ 2

Authors

Rosie M. Walker^{a,b*}, Kadi Vaheer^{a,1}, Mairead L. Bermingham^a, Stewart W. Morris^a, Andrew D. Bretherick^c, Yanni Zeng^{c,2}, Konrad Rawlik^d, Carmen Amador^c, Archie Campbell^e, Chris S. Haley^c, Caroline Hayward^c, David J. Porteous^{a,b,e}, Andrew M. McIntosh^{b,f}, Riccardo E. Marioni^{a,b,3}, Kathryn L. Evans^{a,b,3*}

¹Present address: MRC Centre for Reproductive Health, The Queen's Medical Research Institute, Edinburgh BioQuarter, 47 Little France Crescent, Edinburgh, EH16 4TJ

²Present address: Faculty of Forensic Medicine, Zhongshan School of Medicine, Sun Yat-Sen University, 74 Zhongshan 2nd Road, Guangzhou 510080, China.

³Joint last authors

* Corresponding author: Kathy.Evans@igmm.ed.ac.uk

Affiliations

^aCentre for Genomic and Experimental Medicine, Institute of Genetics and Molecular Medicine, University of Edinburgh, Edinburgh, EH4 2XU, UK

^bCentre for Cognitive Ageing and Cognitive Epidemiology, University of Edinburgh, Edinburgh, EH8 9JZ, UK

^cMRC Human Genetics Unit, Institute of Genetics and Molecular Medicine, University of Edinburgh, Edinburgh, EH4 2XU, UK

^dDivision of Genetics and Genomics, The Roslin Institute and Royal (Dick) School of Veterinary Studies, University of Edinburgh, Easter Bush, Roslin, UK

^eGeneration Scotland, Centre for Genomic and Experimental Medicine, Institute of Genetics and Molecular Medicine, University of Edinburgh, Edinburgh, EH4 2XU, UK

^fDivision of Psychiatry, University of Edinburgh, Royal Edinburgh Hospital, Edinburgh, EH10 5HF, UK

Email addresses

Rosie M. Walker: rwalke13@staffmail.ed.ac.uk; Kadi Vaher: kadi.vaher@ed.ac.uk; Mairead L. Bermingham: mairread.bermingham@igmm.ed.ac.uk, Stewart W. Morris: Stewart.Morris@igmm.ed.ac.uk, Andrew Bretherick: a.bretherick@ed.ac.uk, Yann Zeng: zengyn5@mail.sysu.edu.cn, Konrad Rawlik: Konrad.Rawlik@roslin.ed.ac.uk, Carmen Amador: carmen.amador@igmm.ed.ac.uk, Archie Campbell: archie.campbell@ed.ac.uk, Chris S. Haley: chris.haley@igmm.ed.ac.uk, Caroline Hayward: Caroline.Hayward@igmm.ed.ac.uk, David J. Porteous: david.porteous@igmm.ed.ac.uk, Andrew M. McIntosh: andrew.mcintosh@ed.ac.uk, Riccardo E. Marioni: Riccardo.Marioni@ed.ac.uk, Kathryn L. Evans: Kathy.Evans@igmm.ed.ac.uk

Declarations of interest: AMM has received grant support from Pfizer, Eli Lilly, Janssen and The Sackler Trust. These sources are not connected to the current investigation. AMM has also received speaker fees from Janssen and Illumina. The remaining authors report no conflicts of interest.

Abstract

INTRODUCTION: The *Apolipoprotein E (APOE)* $\epsilon 4$ allele is the strongest genetic risk factor for Alzheimer's disease (AD), while the $\epsilon 2$ allele confers protection. Previous studies report differential DNA methylation of *APOE* between $\epsilon 4$ and $\epsilon 2$ carriers but associations with epigenome-wide methylation are unknown.

METHODS: The EPIC array was used to identify methylation differences between AD-free *APOE* $\epsilon 4$ (n=2469) and $\epsilon 2$ (n=1108) carriers using epigenome-wide association analysis and differentially methylated region (DMR) approaches. Results were explored using pathway and meQTL analyses.

RESULTS: Differentially methylated positions were identified in *APOE*, surrounding genes and genes outside of this locus (*DHCR24*, *LDLR* and *ABCG1*). DMRs were identified in *SREBF2*, *LDLR* and *SQLE*. Pathway and meQTL analyses implicated lipid-related processes; however, blood cholesterol levels could not fully account for the associations.

DISCUSSION: *APOE* $\epsilon 4$ vs. $\epsilon 2$ carrier status is associated with epigenome-wide methylation differences in cis and trans in genes involved in lipid homeostasis.

KEYWORDS: Alzheimer's disease, APOE, Apolipoprotein E, DNA methylation, cholesterol, lipids

1. Introduction

The $\epsilon 4$ allele of the *apolipoprotein E* gene (*APOE*) is the strongest genetic risk factor for late-onset (>65 years) Alzheimer's disease (AD) [1-3]. Inheritance of one copy of this allele increases late-onset AD risk by 2-4-fold, with two copies conferring an 8-12-fold increase in risk compared to the $\epsilon 3/\epsilon 3$ genotype [4, 5]. The $\epsilon 4$ allele is also associated with a younger age-of-onset, with $\epsilon 4$ homozygotes having an average age-of-onset of 68 compared to 84 for $\epsilon 3$ homozygotes [4]. In contrast, the $\epsilon 2$ allele has been associated with a ~50% reduction in AD risk compared to the $\epsilon 3/\epsilon 3$ genotype [5].

The three *APOE* alleles ($\epsilon 2/\epsilon 3/\epsilon 4$) are defined by two *APOE* exon four coding SNPs and encode functionally distinct ApoE isoforms. Isoform-dependent behaviours have been observed for many ApoE functions, including lipid metabolism, Amyloid beta ($A\beta$) metabolism, tau phosphorylation, inflammation, and synaptic plasticity, with ApoE4 and ApoE2 conferring effects consistent with increased and reduced AD risk, respectively [6, 7].

Despite the wealth of evidence linking ApoE to processes implicated in AD pathogenesis, understanding of the specific mechanism(s) by which genetic variation at this locus alters risk remains incomplete. *APOE* genotype acts in conjunction with other genetic and/or environmental factors to confer AD risk: the lifetime risk of dementia or mild cognitive impairment is 31%-40% for $\epsilon 4/\epsilon 4$ homozygotes [8]; and ethnic background and sex modify the effects of *APOE* $\epsilon 4$ [5, 9]. DNA methylation is associated with both genetic and environmental factors, and previous studies have identified associations with AD [10-12], AD risk factors (e.g. ageing [13], obesity [14] and lipid levels [15]), and modifiers of *APOE* genotype effects (e.g. sex [16] and ethnicity [17, 18]).

The two *APOE* haplotype-defining SNPs are located in a CpG island and confer a direct effect on methylation by creating/destroying CpG sites [19]. The *APOE* $\epsilon 2/\epsilon 3/\epsilon 4$ haplotype is associated with methylation at other *APOE* CpGs [20, 21] but, to date, associations with methylation across the epigenome have not been assessed. We hypothesised that characterising these associations would

yield insights into the biological context in which *APOE* acts, thus facilitating the search for mechanisms conferring risk/resilience for AD. Importantly, by studying individuals who are free from AD, we have the potential to identify pathogenic processes that precede the onset of irreversible neurodegeneration.

2. Methods

2.1. Participants

The participants were selected from the Generation Scotland: Scottish Family Health Study (GS:SFHS) cohort (~24,000 participants aged ≥ 18 years at recruitment), which has been described previously [22, 23]. Participants attended a baseline clinical appointment at which they were phenotyped for social, demographic, health and lifestyle factors, completed cognitive assessments, and provided physical measurements and samples for DNA extraction. GS:SFHS obtained ethical approval from the NHS Tayside Committee on Medical Research Ethics, on behalf of the National Health Service (reference: 05/S1401/89) and has Research Tissue Bank Status (reference: 15/ES/0040).

2.2. Blood sample collection and DNA extraction

DNA was extracted from blood (9ml) collected in EDTA tubes using the Nucleon BACC3 Genomic DNA Extraction Kit (Fisher Scientific), following the manufacturer's instructions [24].

2.3. Genotyping of *APOE* and definition of *APOE* $\epsilon 4$ vs. $\epsilon 2$ phenotype

The *APOE* $\epsilon 2/\epsilon 3/\epsilon 4$ haplotypes are defined by two single nucleotide polymorphisms (SNPs), rs429358 and rs7412, which were genotyped using TaqMan probes at the Clinical Research Facility, Edinburgh. A binary variable denoting *APOE* $\epsilon 4$ and $\epsilon 2$ carriers was created by representing *APOE* $\epsilon 4$ carriers with a "1" and *APOE* $\epsilon 2$ with a "0"; $\epsilon 4/\epsilon 2$ and $\epsilon 3/\epsilon 3$ participants were excluded.

2.4. Measurement of cholesterol levels

Total and high-density lipoprotein (HDL) cholesterol were measured at the GS:SFHS baseline appointment and non-HDL cholesterol levels were calculated by subtracting HDL cholesterol from

total cholesterol. The non-HDL cholesterol level reflects a combination of low-density lipoprotein (LDL) cholesterol and very low-density lipoprotein.

2.5. Genome-wide DNA methylation profiling

DNA methylation was profiled using the Infinium MethylationEPIC BeadChip (Illumina Inc.) in a discovery (n=5191) and replication (n=4588) sample, as described previously [25-27] (Supplementary Methods). The discovery and replication samples were normalised separately and converted to M-values. The discovery data was corrected for relatedness (Supplementary Methods). Participants in the replication sample were unrelated (SNP-based relatedness<0.05) to each other and/or discovery sample participants.

Poor performing probes, X/Y chromosome probes and participants with unreliable self-report data or potential XXY genotype were excluded (Supplementary Methods). The final discovery dataset comprised M-values at 777,193 loci for 5087 participants; the replication dataset comprised M-values at 773,860 loci for 4450 participants. The entire discovery sample was used for meQTL analyses whilst subsamples (discovery n=1839; replication n=1738), selected by *APOE* genotype (*APOE* ϵ 4 or ϵ 2 carriers), were assessed in epigenome-wide association studies (EWASs). All subsequent analyses of the DNA methylation data were carried out using R versions 3.6.0. or 3.6.1. [28].

2.6. Statistical analyses

A flow chart indicating all analyses is presented in Figure 1.

2.7. Epigenome-wide association studies

EWASs were implemented using limma [29]. CpG M-values were the dependent variable and *APOE* $\epsilon 4$ vs. $\epsilon 2$ carrier status was the predictor-of-interest. Participants self-reporting AD (n=5) were excluded. Additional covariates were included as below:

Discovery sample

CpG site (pre-corrected for relatedness, estimated cell counts and processing batch) \sim *APOE* $\epsilon 4$ vs. $\epsilon 2$ + age + sex + smoking status + pack years + 20 methylation principal components

Replication sample

CpG site (M-values) \sim *APOE* $\epsilon 4$ vs. $\epsilon 2$ + age + sex + smoking status + pack years + estimated cell counts (granulocytes, natural killer cells, B-lymphocytes, CD4+T-lymphocytes and CD8+T-lymphocytes) + processing batch + 20 methylation principal components

The variables “Smoking status”, “pack years” and the methylation principal components are explained in the Supplementary Methods.

Limma was used to calculate empirical Bayes moderated t-statistics from which *P* values were obtained. The significance threshold in the discovery sample was $P \leq 3.6 \times 10^{-8}$ [30]. Sites attaining significance in the discovery sample were assessed in the replication sample using a Bonferroni-corrected threshold of 0.05/no. sites assessed.

Three additional models were included to assess the effect of co-varying for cholesterol on the relationship between DNA methylation and *APOE* $\epsilon 4$ vs. $\epsilon 2$ carrier status. These models were as above with the exception that either (i) total cholesterol, (ii) HDL cholesterol or (iii) non-HDL cholesterol was included as a covariate.

2.8. EWAS meta-analysis

Inverse standard error-weighted fixed effects meta-analyses of the discovery and replication EWAS results were performed using METAL[31]. Sites attaining a meta-analysis $P \leq 3.6 \times 10^{-8}$ were considered significant.

2.9. Identification of differentially methylated regions

Differentially methylated regions (DMRs) associated with *APOE* $\epsilon 4$ vs. $\epsilon 2$ carrier status were identified using the `dmrff.meta` function from the `dmrff` R package[32]. DMRs were defined as regions containing 2-30 sites separated ≤ 500 bp with EWAS meta-analysis P values $\leq .05$ and methylation changes in a consistent direction. DMRs with Bonferroni-adjusted P values $\leq .05$ were declared significant.

2.10. Gene ontology/KEGG pathway analyses

Gene ontology (GO) and KEGG pathway analyses were implemented using a modified version of `missMethyl`'s `gometh` function [33] (Supplementary Methods). The target list comprised probes associated with the phenotype-of-interest ($P \leq 1 \times 10^{-5}$) in the meta-EWAS or DMR analysis and the gene universe included all analysed probe. Enrichment was assessed using a hypergeometric test, accounting for the bias arising from the variation in the number of probes-per-gene. Bonferroni-corrected significance thresholds of $P \leq 2.88 \times 10^{-6}$ and $P \leq 1.50 \times 10^{-4}$ were applied to account for the 17,344 GO terms and 333 KEGG pathways assessed.

2.11. Genotyping and imputation

The genotyping and imputation of GS:SFHS has been described previously [24, 34] (Supplementary Methods).

2.12. Identification of methylation quantitative trait loci

Methylation quantitative trait loci were identified using the discovery sample (Bretherick et al., in preparation). Following quality control (described in 2.6), the data was normalised and corrected as described previously [35] (Supplementary Methods). Normalised and corrected data was available for 27 of the 31 CpGs-of-interest in this study. The resulting residuals were inverse rank transformed and entered as the dependent variable in simple linear model GWASs to identify meQTLs. SNPs that were associated with a CpG with $P \leq 1.85 \times 10^{-9}$ ($5 \times 10^{-8}/27$) were declared to be meQTLs.

2.13. Genome-wide association study of *APOE* $\epsilon 4$ vs. $\epsilon 2$ carrier status

Association tests used BOLT-LMM [36] to perform linear mixed models in participants with available *APOE* genotypes ($\epsilon 2$ n=2613; $\epsilon 4$ n=5401). BOLT-LMM adjusts for population structure and relatedness between individuals whilst assessing association. Sex was included as a covariate. Associations were considered significant when $P \leq 5 \times 10^{-8}$.

3. Results

3.1. EWAS sample demographics

The discovery sample comprised 1253 *APOE* ϵ 4 and 586 *APOE* ϵ 2 allele carriers and the replication sample comprised 1216 *APOE* ϵ 4 and 522 *APOE* ϵ 2 allele carriers. Key sample demographic information is presented in Supplementary Table 1.

3.2. Identification of differentially methylated positions and regions in *APOE* ϵ 4 vs. ϵ 2 carriers

An EWAS of *APOE* ϵ 4 vs. ϵ 2 carriers in the discovery sample identified eight significantly differentially methylated positions (DMPs; $1.56 \times 10^{-56} \leq P \leq 8.80 \times 10^{-9}$). All eight sites were also significant ($8.83 \times 10^{-49} \leq P \leq 7.27 \times 10^{-6}$) in the replication sample with a consistent direction of effect (Supplementary Table 2). The eight sites are located in a ~169kb region on chromosome 19 (chr. 19: 45,242,346-45,411,802; GRCh37/hg19), which spans a region of the genome upstream of and including part of the *APOE* gene (chr19: 45,409,039-45,412,650; GRCh37/hg19).

Inverse standard error-weighted fixed effects meta-analysis of the discovery and replication samples identified 20 DMPs, including the eight replicated sites, ($2.59 \times 10^{-100} \leq P \leq 2.44 \times 10^{-8}$; Table 1; Figure 2). Sixteen of these sites are located on chromosome 19q in a ~233kb region (chr19: 45,221,584 – 45,454,752; GRCh37/hg19) encompassing *APOE* and several surrounding genes (Supplementary Figure 1). Henceforth, the region containing *APOE* and neighbouring genes will be referred to as the “*APOE* locus”. The most significant DMP, cg13375295, is located ~4.5kb upstream of *Poliovirus Receptor-related 2 (PVRL2)*, a gene situated ~16.5kb upstream of *APOE*. Four other DMPs (cg10762466, cg10178308, cg11643040 and cg06198803) are located either upstream or in the gene body of *PVRL2*. Two DMPs (cg06750524 and cg16471933) are located in *APOE*: cg06750524, the DMP with the largest effect size, in the intron between exons 2 and 3; and cg16471933 in exon four, 139bp 5' of rs429358, one of the *APOE* ϵ 4/ ϵ 2-defining SNPs. Although both the *APOE* DMPs are

more highly methylated in *APOE* $\epsilon 4$ carriers; the DMPs in the surrounding region do not show a consistent direction of effect.

Four DMPs are located outside of chromosome 19q: cg17901584 on chromosome 1, 785bp upstream of the *24-dehydrocholesterol reductase (DHCR24)* gene; cg19751789, 94bp upstream of the *low density lipoprotein receptor (LDLR)* gene on chromosome 19p; and two, cg16740586 and cg06500161, are located 668bp apart in the same intron of multiple *ATP Binding Cassette Subfamily G Member 1 (ABCG1)* isoforms.

Differentially methylated regions (DMRs) were identified using a meta-analysis approach, which identified four significant regions, none of which are located at the *APOE* locus (Table 2). Two are in the first intron of *Sterol Regulatory Element Binding Transcription Factor 2 (SREBF2)*, while the others are in the putative promoter of *LDLR* (spanning a 93bp region 94bp upstream of the *LDLR* transcription start site) and the first exon and intron of *Squalene Epoxidase (SQLE)* (Figure 1). All four DMRs are hypomethylated in *APOE* $\epsilon 4$ carriers. Only the *LDLR* DMR contains a site that was identified as a DMP (cg19751789).

GO analysis was carried out using the 23 Entrez IDs mapping to the 49 probes with a meta-EWAS or DMR analysis $P \leq 1 \times 10^{-5}$. This identified 14 significant GO terms (Table 3), the most significant of which was “chylomicron remnant clearance” ($P=6.02 \times 10^{-11}$). Significant enrichment for the KEGG pathways “cholesterol metabolism” ($P=1.89 \times 10^{-9}$) and “steroid biosynthesis” ($P=1.95 \times 10^{-4}$) was also observed.

3.3. Assessment of the role of cholesterol in mediating methylation differences between *APOE* $\epsilon 4$ and $\epsilon 2$ carriers

Given the well-established role of ApoE in cholesterol metabolism [6], the effects of co-varying for cholesterol levels (total, HDL or non-HDL cholesterol) on the association between *APOE* $\epsilon 4$ vs. $\epsilon 2$

carrier status and the 20 meta-analysis-identified DMPs were assessed (Supplementary Table 3). In general, small changes in effect sizes were observed (10, 17, and 13 probes showed mean decreases of 3.2%, 4.68%, and 5.10% when co-varying for total, HDL, and non-HDL cholesterol, respectively). Six DMPs (four at the *APOE* locus and two outside of this region) were no longer significant ($4.03 \times 10^{-8} \leq P \leq 4.77 \times 10^{-6}$) after co-varying for at least one cholesterol measure.

3.4. Assessment of meQTLs associated with loci that are differentially methylated between *APOE* $\epsilon 4$ and $\epsilon 2$ carriers

To explore the DMP and DMR CpGs further, the results of meQTL analyses previously carried out in this dataset (Bretherick et al., in preparation) were queried. It was possible to assess meQTLs for 27 of the 31 CpGs of interest (from the DMP and DMR analyses). Amongst these CpGs, 25 were associated with a meQTL. In total, 4573 significant CpG-SNP associations were identified for the 25 CpGs, involving 1974 unique SNPs (Figure 3; Supplementary Table 4). Almost half of the meQTLs ($n=947$) were located in a ~ 719 kb region (chr19: 45,004,645– 45,723,446; GRCh37/hg19) spanning *APOE*. These meQTLs are associated with 15 CpGs, of which 13 are located at the *APOE* locus. No single meQTL is associated with all 15 CpGs: two are each associated with nine CpGs: rs7412 one of the *APOE* $\epsilon 2/\epsilon 3/\epsilon 4$ -defining SNPs; and rs41290120, an intronic *PVRL2* SNP that is in LD with rs7412 with $D' = 0.85$ in the British population [37]. The two CpGs associated in *trans* are cg16000331 in *SREBF2* and cg19751789 in *LDLR*.

Outside of the *APOE* locus, the remaining 1027 meQTLs, which are associated with 13 CpGs, are located in 12 genomic regions (Figure 3; Supplementary Table 5), with each meQTL region containing meQTLs associated with between one and nine CpGs-of-interest. To assess whether these meQTLs might contribute to *APOE* $\epsilon 4$ vs. $\epsilon 2$ -associated methylation differences, their association with *APOE* $\epsilon 4$ vs. $\epsilon 2$ carrier status was assessed. No significant associations were observed, suggesting that the

APOE $\epsilon 4$ vs. $\epsilon 2$ -associated methylation differences are predominantly driven by effects at the *APOE* locus.

To investigate potential trait/disease associations with variation in methylation levels at the CpGs-of-interest, the GWAS catalog was queried. This identified 188/1974 meQTLs as having genome-wide significant associations with 244 traits (Supplementary Table 6). More than one third of the associations are with a lipid-related trait. Outside of the *APOE* locus, four SNPs, located in a region encompassing the 3' end of *CCDC134* and most of the neighbouring *SREBF2*, have been associated with cognitive ability-related traits. Between them, these four SNPs are associated in *cis* with methylation at the four CpGs forming the two *SREBF2* DMRs.

Discussion

We performed the first genome-wide comparison of DNA methylation between carriers of the *APOE* $\epsilon 4$ and $\epsilon 2$ haplotypes, which confer risk for and protection from AD, respectively. In a large population-based cohort, we identified several CpGs showing methylation differences at the *APOE* locus (i.e. *APOE* and neighbouring genes) and outside of this locus in genes implicated in lipid homeostasis.

Methylation differences were identified using test, replication and meta-analysis EWASs and DMR analysis. Eight DMPs located on chromosome 19 in a ~169kb region spanning from upstream of *BCL3* to the *APOE*'s fourth exon showed replicated association. An additional 12 DMPs, 8 of which are located in a ~233kb region at the *APOE* locus, were identified by meta-analysing the discovery and replication samples. DMR analysis identified four regions of differential methylation, all of which are located outside of the *APOE* locus.

Within the *APOE* gene, two DMPs, cg06750524, in the second intron, and cg16471933, in the fourth exon, were identified. *APOE* $\epsilon 4$ carriers showed higher methylation levels at both. This observation directly replicates a previous study [21] and is in line with Foraker et al.'s observation of increased methylation of the *APOE* exon four CpG island in $\epsilon 4$ carriers [20]. The CpG sites that are created/destroyed by the two *APOE* $\epsilon 2/\epsilon 3/\epsilon 4$ -defining SNPs were not profiled in this study; however, the $\epsilon 4$ haplotype adds a CpG site and the $\epsilon 2$ haplotype removes a CpG site compared to the $\epsilon 3$ haplotype [19]. These observations suggest a general trend for increased *APOE* methylation in $\epsilon 4$ carriers. A further 11 *APOE* CpGs assessed in this study were not found to be differentially methylated; however inspection of the coefficients for these sites indicates that eight showed increased methylation in $\epsilon 4$ carriers in both the discovery and replication EWAS samples.

The differentially methylated CpGs at the *APOE* locus span a broad region that contains several genes containing AD-associated variants [38]. Long-ranging linkage disequilibrium in the region

complicates the interpretation of association signals; however, conditional analysis suggests the presence of multiple independent AD risk loci [3]. As such, the methylation differences observed in this study may be associated with variants in LD with the *APOE* $\epsilon 2/\epsilon 4$ -defining SNPs, which may be independent risk loci. It is beyond the scope of the current study to investigate this possibility but this should be addressed by future studies.

Beyond the *APOE* locus, DMPs were identified in an *ABCG1* intron, and upstream of *DHCR24* and *LDLR*; DMRs were identified in the gene bodies of *SREBF2* and *SQLE*, and in the putative promoter region of *LDLR*. Although these CpGs are associated with several meQTLs, located both within and outside of the *APOE* locus, assessment of the association between the meQTLs and *APOE* $\epsilon 4$ vs. $\epsilon 2$ carrier status suggested that the observed methylation differences are not attributable to allelic association between *cis* meQTLs and *APOE* $\epsilon 4/\epsilon 2$ haplotype.

The genes outside of the *APOE* locus that harbour differentially methylation CpGs are implicated in lipid metabolism or homeostasis. *ABCG1*, which is highly expressed in the brain, encodes a cholesterol and phospholipid transporter and is involved in regulating the sterol biosynthetic pathway[39]. *DHCR24*, which encodes the cholesterol biosynthesis enzyme 3 β -hydroxysterol- $\Delta 24$ reductase, plays a neuroprotective role in AD-related stress conditions, including A β toxicity, oxidative stress and inflammation[40, 41]. The *LDLR* gene encodes the LDL receptor, one of the neuronal receptors capable of mediating the endocytosis of ApoE and, thus, maintaining brain cholesterol homeostasis. *LDLR* expression is regulated, in part, by *SREBF2*, a transcriptional regulator of sterol-regulated genes, which contains a SNP that is associated both with *SREBF2* expression and CSF levels of the AD biomarkers A β and tau [42]. *SQLE* encodes squalene monooxygenase, a rate-limiting catalyst in sterol biosynthesis.

The link between *APOE* $\epsilon 4$ vs. $\epsilon 2$ -associated methylation differences and lipid-related processes and pathways was further supported by GO and KEGG analyses, the identification of meQTLs for the

differentially methylated CpGs and their GWAS-associated phenotypes. Previous EWASs have also identified associations between some of the *APOE* $\epsilon 4$ vs. $\epsilon 2$ -associated CpGs and cholesterol levels: the *DHCR24* (cg17901584), *ABCG1* (cg06500161) and *SREBF2* (cg16000331) DMPs have been associated with HDL cholesterol, total cholesterol and triglyceride levels[15, 43-45]. Comparisons with previous EWASs are, however, limited by the fact that majority of previous EWASs used the 450K array, which, does not contain 10 of the *APOE* $\epsilon 4$ vs. $\epsilon 2$ -associated CpGs. Differences in lipid metabolism between carriers of the *APOE* $\epsilon 4$ and $\epsilon 2$ haplotypes are well-documented and have been proposed to contribute to AD pathogenesis through multiple mechanisms, including effecting $A\beta$ processing [6].

These observations raise the question of the nature of the causal relationship between *APOE* $\epsilon 4$ vs. $\epsilon 2$ -associated variation in methylation and lipid metabolism. Although the present study does not address this question directly, we assessed whether variation in blood cholesterol levels could account for the observed methylation differences. Co-varying for either total, HDL, or non-HDL blood cholesterol levels resulted in a decrease in the effect size of the $\epsilon 4$ vs. $\epsilon 2$ association for a subset of the probes, with the HDL cholesterol affecting the most probes (17/20); however, the magnitude of the decrease was small (~5%), suggesting that variation in cholesterol levels cannot fully account for the observed methylation differences. Limitations to the GS:SFHS cholesterol data should, however, be noted: triglyceride levels were not measured, preventing LDL cholesterol assessment; and blood samples were not taken at a consistent time of day or after fasting.

The cross-sectional nature of the present study precludes the observed differences being interpreted as conferring risk, protection or compensation. Comparison of methylation at these loci in *APOE* $\epsilon 4$ and $\epsilon 2$ carriers with AD would be useful in addressing this question; however, the optimum study design would involve the longitudinal assessment of the trajectory of $\epsilon 4$ vs. $\epsilon 2$ -associated methylation differences in AD-free individuals in midlife who either do or do not later develop AD. Moreover, the present study was limited to studying DNA methylation in blood.

Although peripheral processes play a role in conferring risk for AD [46], it would be of interest to assess *APOE* genotype-associated methylation differences in the brain.

This is the first study to characterise epigenome-wide DNA methylation differences between carriers of *APOE* $\epsilon 4$ and $\epsilon 2$. In AD-free individuals, we identified several methylation differences both at the *APOE* locus and in the rest of the genome, which converge on lipid-related pathways. Strengths of the study include the large sample available for EWAS analysis, the epigenome-wide approach, the use of a well-phenotyped cohort with genotype data, and the avoidance of reverse causation by studying AD-free participants. Future studies should investigate the causal relationship between *APOE* genotype, DNA methylation and lipid-related processes and their role in AD pathogenesis.

Acknowledgements

This work was supported by a Wellcome Trust Strategic Award “Stratifying Resilience and Depression Longitudinally” (STRADL) [104036/Z/14/Z] to AMM, KLE, CSH, DJP and others, and an MRC Mental Health Data Pathfinder Grant [MC_PC_17209] to AMM and DJP. REM is supported by an Alzheimer’s Research UK major project grant [ARUK-PG2017B-10]. KV is funded by the Wellcome Trust Translational Neuroscience PhD Programme at the University of Edinburgh [108890/Z/15/Z]. ADB would like to acknowledge funding from the Wellcome PhD training fellowship for clinicians [204979/Z/16/Z], the Edinburgh Clinical Academic Track (ECAT) programme. Generation Scotland received core support from the Chief Scientist Office of the Scottish Government Health Directorates [CZD/16/6] and the Scottish Funding Council [HR03006]. Genotyping of the GS:SFHS samples was carried out by the Genetics Core Laboratory at the Clinical Research Facility, Edinburgh, Scotland and was funded by the UK’s Medical Research Council and the Wellcome Trust [104036/Z/14/Z]. DNA methylation profiling of the GS:SFHS samples was funded by the Wellcome Trust Strategic Award [10436/Z/14/Z]. RMW, AMM, DJP, REM and KLE are members of The University of Edinburgh Centre for Cognitive Ageing and Cognitive Epidemiology (CCACE), part of the cross-council Lifelong Health and Wellbeing Initiative [MR/K026992/1]. Funding for CCACE from the Biotechnology and Biological Sciences Research Council and Medical Research Council is gratefully acknowledged.

We are grateful to all the families who took part, the general practitioners and the Scottish School of Primary Care for their help in recruiting them, and the whole Generation Scotland team, which includes interviewers, computer and laboratory technicians, clerical workers, research scientists, volunteers, managers, receptionists, healthcare assistants and nurses.

References

- [1] Lambert JC, Ibrahim-Verbaas CA, Harold D, Naj AC, Sims R, Bellenguez C, et al. Meta-analysis of 74,046 individuals identifies 11 new susceptibility loci for Alzheimer's disease. *Nat Genet.* 2013;45:1452-8.
- [2] Kunkle BW, Grenier-Boley B, Sims R, Bis JC, Damotte V, Naj AC, et al. Genetic meta-analysis of diagnosed Alzheimer's disease identifies new risk loci and implicates Abeta, tau, immunity and lipid processing. *Nat Genet.* 2019;51:414-30.
- [3] Jansen IE, Savage JE, Watanabe K, Bryois J, Williams DM, Steinberg S, et al. Genome-wide meta-analysis identifies new loci and functional pathways influencing Alzheimer's disease risk. *Nat Genet.* 2019;51:404-13.
- [4] Corder EH, Saunders AM, Strittmatter WJ, Schmechel DE, Gaskell PC, Small GW, et al. Gene dose of apolipoprotein E type 4 allele and the risk of Alzheimer's disease in late onset families. *Science.* 1993;261:921-3.
- [5] Farrer LA, Cupples LA, Haines JL, Hyman B, Kukull WA, Mayeux R, et al. Effects of age, sex, and ethnicity on the association between apolipoprotein E genotype and Alzheimer disease. A meta-analysis. APOE and Alzheimer Disease Meta Analysis Consortium. *JAMA.* 1997;278:1349-56.
- [6] Safieh M, Korczyn AD, Michaelson DM. ApoE4: an emerging therapeutic target for Alzheimer's disease. *BMC Med.* 2019;17:64.
- [7] Tzioras M, Davies C, Newman A, Jackson R, Spires-Jones T. Invited Review: APOE at the interface of inflammation, neurodegeneration and pathological protein spread in Alzheimer's disease. *Neuropathol Appl Neurobiol.* 2019;45:327-46.
- [8] Qian J, Wolters FJ, Beiser A, Haan M, Ikram MA, Karlawish J, et al. APOE-related risk of mild cognitive impairment and dementia for prevention trials: An analysis of four cohorts. *PLoS Med.* 2017;14:e1002254.
- [9] Babenko VN, Afonnikov DA, Ignatieva EV, Klimov AV, Gusev FE, Rogaev EI. Haplotype analysis of APOE intragenic SNPs. *BMC Neurosci.* 2018;19:16.

- [10] De Jager PL, Srivastava G, Lunnon K, Burgess J, Schalkwyk LC, Yu L, et al. Alzheimer's disease: early alterations in brain DNA methylation at ANK1, BIN1, RHBDF2 and other loci. *Nat Neurosci*. 2014;17:1156-63.
- [11] Gasparoni G, Bultmann S, Lutsik P, Kraus TFJ, Sordon S, Vlcek J, et al. DNA methylation analysis on purified neurons and glia dissects age and Alzheimer's disease-specific changes in the human cortex. *Epigenetics Chromatin*. 2018;11:41.
- [12] Lunnon K, Smith R, Hannon E, De Jager PL, Srivastava G, Volta M, et al. Methylomic profiling implicates cortical deregulation of ANK1 in Alzheimer's disease. *Nat Neurosci*. 2014;17:1164-70.
- [13] Slieker RC, Relton CL, Gaunt TR, Slagboom PE, Heijmans BT. Age-related DNA methylation changes are tissue-specific with ELOVL2 promoter methylation as exception. *Epigenetics Chromatin*. 2018;11:25.
- [14] Wahl S, Drong A, Lehne B, Loh M, Scott WR, Kunze S, et al. Epigenome-wide association study of body mass index, and the adverse outcomes of adiposity. *Nature*. 2017;541:81-6.
- [15] Hedman AK, Mendelson MM, Marioni RE, Gustafsson S, Joehanes R, Irvin MR, et al. Epigenetic Patterns in Blood Associated With Lipid Traits Predict Incident Coronary Heart Disease Events and Are Enriched for Results From Genome-Wide Association Studies. *Circ Cardiovasc Genet*. 2017;10.
- [16] Singmann P, Shem-Tov D, Wahl S, Grallert H, Fiorito G, Shin SY, et al. Characterization of whole-genome autosomal differences of DNA methylation between men and women. *Epigenetics Chromatin*. 2015;8:43.
- [17] Galanter JM, Gignoux CR, Oh SS, Torgerson D, Pino-Yanes M, Thakur N, et al. Differential methylation between ethnic sub-groups reflects the effect of genetic ancestry and environmental exposures. *Elife*. 2017;6.
- [18] Yuan V, Price EM, Del Gobbo G, Mostafavi S, Cox B, Binder AM, et al. Accurate ethnicity prediction from placental DNA methylation data. *Epigenetics Chromatin*. 2019;12:51.
- [19] Yu CE, Cudaback E, Foraker J, Thomson Z, Leong L, Lutz F, et al. Epigenetic signature and enhancer activity of the human APOE gene. *Hum Mol Genet*. 2013;22:5036-47.

- [20] Foraker J, Millard SP, Leong L, Thomson Z, Chen S, Keene CD, et al. The APOE Gene is Differentially Methylated in Alzheimer's Disease. *J Alzheimers Dis.* 2015;48:745-55.
- [21] Ma Y, Smith CE, Lai CQ, Irvin MR, Parnell LD, Lee YC, et al. Genetic variants modify the effect of age on APOE methylation in the Genetics of Lipid Lowering Drugs and Diet Network study. *Aging Cell.* 2015;14:49-59.
- [22] Smith BH, Campbell A, Linksted P, Fitzpatrick B, Jackson C, Kerr SM, et al. Cohort Profile: Generation Scotland: Scottish Family Health Study (GS:SFHS). The study, its participants and their potential for genetic research on health and illness. *Int J Epidemiol.* 2013;42:689-700.
- [23] Smith BH, Campbell H, Blackwood D, Connell J, Connor M, Deary IJ, et al. Generation Scotland: the Scottish Family Health Study; a new resource for researching genes and heritability. *BMC medical genetics.* 2006;7:74.
- [24] Kerr SM, Campbell A, Murphy L, Hayward C, Jackson C, Wain LV, et al. Pedigree and genotyping quality analyses of over 10,000 DNA samples from the Generation Scotland: Scottish Family Health Study. *BMC medical genetics.* 2013;14:38.
- [25] Barbu MC, Walker RM, Howard DM, Evans KL, Whalley HC, Porteous DJ, et al. Epigenetic prediction of major depressive disorder. *medRxiv.* 2019:19001123.
- [26] Madden RA, McCartney DL, Walker RM, Hillary RF, Bermingham ML, Rawlik K, et al. Birth weight predicts psychiatric and physical health, cognitive function, and DNA methylation differences in an adult population. *bioRxiv.* 2019:664045.
- [27] Bermingham ML, Walker RM, Marioni RE, Morris SW, Rawlik K, Zeng Y, et al. Identification of novel differentially methylated sites with potential as clinical predictors of impaired respiratory function and COPD. *EBioMedicine.* 2019;43:576-86.
- [28] Team RC. R: A language and environment for statistical computing. Vienna, Austria: R Foundation for Statistical Computing; 2019.
- [29] Ritchie ME, Phipson B, Wu D, Hu Y, Law CW, Shi W, et al. limma powers differential expression analyses for RNA-sequencing and microarray studies. *Nucleic Acids Res.* 2015;43:e47.

- [30] Saffari A, Silver MJ, Zavattari P, Moi L, Columbano A, Meaburn EL, et al. Estimation of a significance threshold for epigenome-wide association studies. *Genet Epidemiol.* 2018;42:20-33.
- [31] Willer CJ, Li Y, Abecasis GR. METAL: fast and efficient meta-analysis of genomewide association scans. *Bioinformatics.* 2010;26:2190-1.
- [32] Suderman M, Staley JR, French R, Arathimos R, Simpkin A, Tilling K. dmrff: identifying differentially methylated regions efficiently with power and control. *bioRxiv.* 2018:508556.
- [33] Phipson B, Maksimovic J, Oshlack A. missMethyl: an R package for analyzing data from Illumina's HumanMethylation450 platform. *Bioinformatics.* 2016;32:286-8.
- [34] Nagy R, Boutin TS, Marten J, Huffman JE, Kerr SM, Campbell A, et al. Exploration of haplotype research consortium imputation for genome-wide association studies in 20,032 Generation Scotland participants. *Genome Med.* 2017;9:23.
- [35] Zeng Y, Amador C, Xia C, Marioni R, Sproul D, Walker RM, et al. Parent of origin genetic effects on methylation in humans are common and influence complex trait variation. *Nat Commun.* 2019;10:1383.
- [36] Loh PR, Tucker G, Bulik-Sullivan BK, Vilhjalmsdottir BJ, Finucane HK, Salem RM, et al. Efficient Bayesian mixed-model analysis increases association power in large cohorts. *Nat Genet.* 2015;47:284-90.
- [37] Machiela MJ, Chanock SJ. LDlink: a web-based application for exploring population-specific haplotype structure and linking correlated alleles of possible functional variants. *Bioinformatics.* 2015;31:3555-7.
- [38] Zhou X, Chen Y, Mok KY, Kwok TCY, Mok VCT, Guo Q, et al. Non-coding variability at the APOE locus contributes to the Alzheimer's risk. *Nat Commun.* 2019;10:3310.
- [39] Burgess BL, Parkinson PF, Racke MM, Hirsch-Reinshagen V, Fan J, Wong C, et al. ABCG1 influences the brain cholesterol biosynthetic pathway but does not affect amyloid precursor protein or apolipoprotein E metabolism in vivo. *J Lipid Res.* 2008;49:1254-67.

- [40] Greeve I, Hermans-Borgmeyer I, Brellinger C, Kasper D, Gomez-Isla T, Behl C, et al. The human DIMINUTO/DWARF1 homolog seladin-1 confers resistance to Alzheimer's disease-associated neurodegeneration and oxidative stress. *J Neurosci*. 2000;20:7345-52.
- [41] Martiskainen H, Paldanius KMA, Natunen T, Takalo M, Marttinen M, Leskela S, et al. DHCR24 exerts neuroprotection upon inflammation-induced neuronal death. *J Neuroinflammation*. 2017;14:215.
- [42] Picard C, Julien C, Frappier J, Miron J, Theroux L, Dea D, et al. Alterations in cholesterol metabolism-related genes in sporadic Alzheimer's disease. *Neurobiol Aging*. 2018;66:180 e1- e9.
- [43] Braun KVE, Dhana K, de Vries PS, Voortman T, van Meurs JBJ, Uitterlinden AG, et al. Epigenome-wide association study (EWAS) on lipids: the Rotterdam Study. *Clin Epigenetics*. 2017;9:15.
- [44] Pfeiffer L, Wahl S, Pilling LC, Reischl E, Sandling JK, Kunze S, et al. DNA methylation of lipid-related genes affects blood lipid levels. *Circ Cardiovasc Genet*. 2015;8:334-42.
- [45] Sayols-Baixeras S, Subirana I, Lluís-Ganella C, Civeira F, Roquer J, Do AN, et al. Identification and validation of seven new loci showing differential DNA methylation related to serum lipid profile: an epigenome-wide approach. The REGICOR study. *Hum Mol Genet*. 2016;25:4556-65.
- [46] Morris G, Berk M, Maes M, Puri BK. Could Alzheimer's Disease Originate in the Periphery and If So How So? *Mol Neurobiol*. 2019;56:406-34.

- 1 **Table 1.** Significant DMPs identified in an inverse standard error-weighted meta-analysis of results
- 2 from the discovery and replication EWASs comparing *APOE* ε4 and ε2 allele carriers

Probe ID	Gene symbol	Gene feature *	Chr.	BP [†]	Effect [‡]	SE	P value
cg13375295			19	45344725	-0.1031	0.0049	2.59 x 10 ⁻¹⁰⁰
cg06750524	<i>APOE</i>	Body	19	45409955	0.1122	0.008	1.07 x 10 ⁻⁴⁴
cg16094954	<i>BCL3</i>	TSS1500	19	45251180	-0.0994	0.0081	8.24 x 10 ⁻³⁵
cg10762466			19	45347693	-0.0463	0.004	1.33 x 10 ⁻³⁰
cg16471933	<i>APOE</i>	Body	19	45411802	0.0606	0.0055	7.20 x 10 ⁻²⁸
cg10178308	<i>PVRL2</i>	TSS200	19	45349383	0.1075	0.0103	2.09 x 10 ⁻²⁵
cg27087650	<i>BCL3</i>	Body	19	45255796	0.0455	0.0044	3.74 x 10 ⁻²⁵
cg04488858			19	45242346	-0.0514	0.0065	2.28 x 10 ⁻¹⁵
cg11643040	<i>PVRL2</i>	Body	19	45361327	-0.0278	0.0038	1.44 x 10 ⁻¹³
cg26631131			19	45240591	0.0298	0.0042	2.45 x 10 ⁻¹²
cg17901584	<i>DHCR24;RP11-67L3.4</i>	TSS1500	1	55353706	-0.0403	0.0058	3.58 x 10 ⁻¹²
cg06198803	<i>PVRL2</i>	Body	19	45371896	-0.041	0.006	1.04 x 10 ⁻¹¹
cg16740586	<i>ABCG1</i>	Body	21	43655919	0.0332	0.005	3.58 x 10 ⁻¹¹
cg03793277	<i>APOC1</i>	TSS1500	19	45416910	-0.0304	0.0049	5.91 x 10 ⁻¹⁰
cg06500161	<i>ABCG1</i>	Body	21	43656587	0.0247	0.0042	2.65 x 10 ⁻⁹
cg09555818	<i>APOC2;APOC4</i>	5' UTR; 1 st exon	19	45449301	-0.0531	0.0091	5.79 x 10 ⁻⁹
cg13119609	<i>APOC2;APOC4</i>	5' UTR; 1 st exon	19	45449297	-0.0464	0.008	5.86 x 10 ⁻⁹

cg15233575			19	45221584	-0.0223	0.0039	7.04×10^{-9}
cg14645843			19	45454752	-0.0346	0.0062	2.31×10^{-8}
cg19751789	<i>LDLR</i>		19	11199944	-0.0338	0.0061	2.44×10^{-8}

3

4 Abbreviations: BP, base position; Chr., chromosome; SE, standard error; TSS, transcription start site;

5 UTR, untranslated region

6 * Gene feature: 5' UTR: between the TSS and the ATG; Body: between the ATG and the stop codon;

7 TSS200: within 200 bases 5' of the TSS; TSS1500: within 1500 bases 5' of the TSS.

8 † Base position in genome assembly hg19/GRCh37

9 ‡ Effect direction is relative to carriers of the $\epsilon 2$ allele

10 **Table 2.** Significant DMRs identified through DMR meta-analysis of the discovery and replication

11 sample EWAS results

Chr.	Coordinates*	Gene symbol	Effect [†]	SE	Adj. P value [‡]	CpGs
19	11199851- 11199944	<i>LDLR</i>	-0.026	0.004	0.001474	cg19751789; cg07960944; cg22381454; cg05249393; cg18596381
22	42229983- 42230138	<i>SREBF2</i>	-0.027	0.005	0.008988	cg09978077; cg16000331
22	42230879- 42230899	<i>SREBF2</i>	-0.034	0.006	0.017317	cg15128785; cg12403973
8	126011784- 126012434	<i>SQLE</i>	-0.031	0.006	0.021819	cg09984392; cg00285394; cg14660676

12

13 Abbreviations: Chr., chromosome; SE, standard error; Adj., adjusted; CpGs, cytosine and guanine

14 nucleotides linked by a phosphate bond

15 * DMR start and end coordinates in genome assembly hg19/GRCh37

16 [†]Effect direction is relative to carriers of the $\epsilon 2$ allele

17 [‡]Bonferroni-adjusted P value

18

19 **Table 3.** GO terms showing significant enrichment for probes showing differences in methylation
 20 between *APOE* ε4 and *APOE* ε2 carriers

Ontology category	GO term	Proportion *	P value
BP	chylomicron remnant clearance	4/8	6.02 x 10 ⁻¹¹
CC	very-low-density lipoprotein particle	8/20	3.96 x 10 ⁻⁹
BP	cholesterol homeostasis	6/91	1.81 x 10 ⁻⁸
BP	very-low-density lipoprotein particle clearance	3/6	2.31 x 10 ⁻⁸
BP	high-density lipoprotein particle clearance	3/10	1.04 x 10 ⁻⁷
BP	phospholipid efflux	4/11	1.52 x 10 ⁻⁷
CC	Chylomicron	3/12	2.17 x 10 ⁻⁷
CC	low-density lipoprotein particle	3/14	3.15 x 10 ⁻⁷
BP	cholesterol metabolic process	5/62	6.02 x 10 ⁻⁷
BP	high-density lipoprotein particle remodelling	4/17	7.06 x 10 ⁻⁷
CC	high-density lipoprotein particle	3/22	1.11 x 10 ⁻⁶
BP	response to caloric restriction	2/2	1.40 x 10 ⁻⁶
BP	cholesterol efflux	4/22	1.75 x 10 ⁻⁶
BP	triglyceride homeostasis	3/29	2.63 x 10 ⁻⁶

21

22 Abbreviations: BP, biological process; CC, cellular component; GO, gene ontology; MF, molecular

23 function

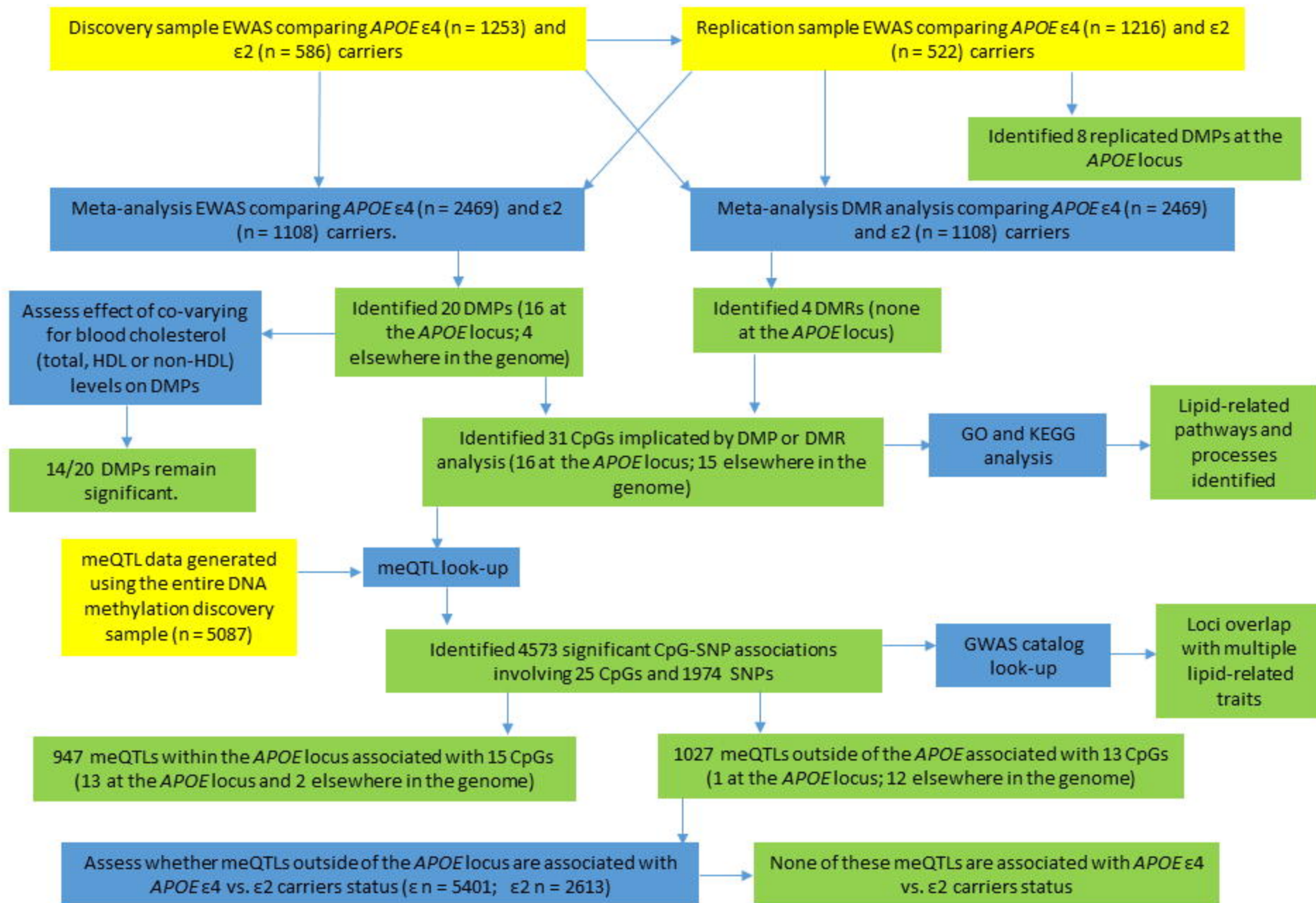
- 24 * Number of significant target list-associated Entrez IDs associated with the gene ontology term /total
- 25 number of Entrez IDs associated with the GO term. The target list comprised probes that met a
- 26 nominal threshold for association with *APOE* ε4 vs. ε2 carrier status of $P \leq 1 \times 10^{-5}$.

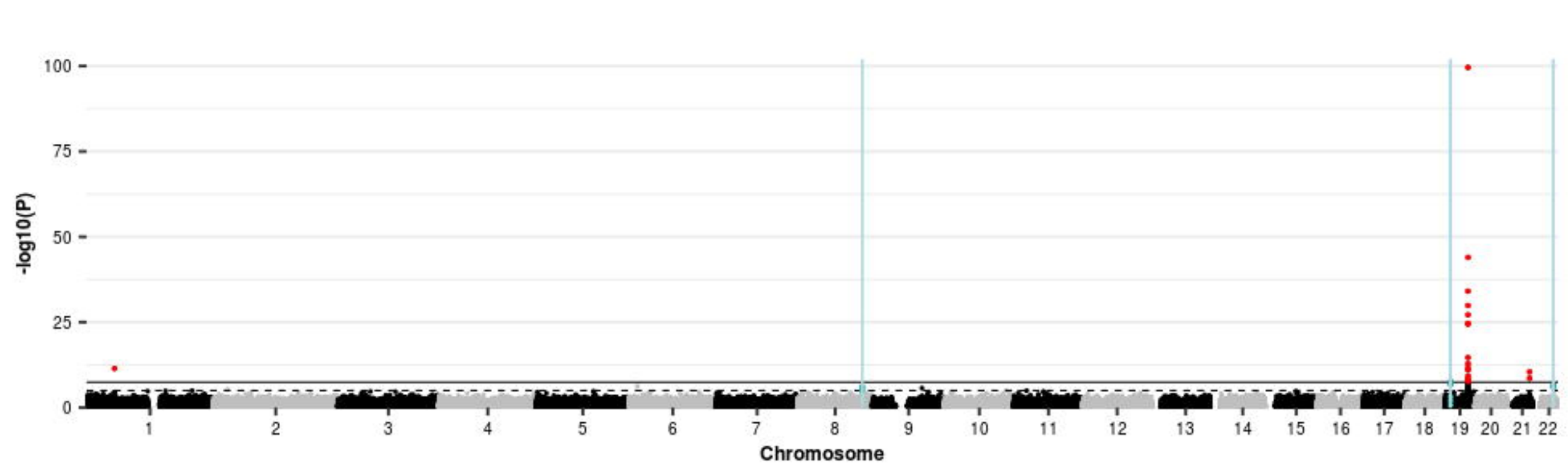
27 Figure legends

28 **Figure 1.** Flow chart indicating the analyses carried out in this study. Yellow boxes indicate datasets
29 used for the analysis, blue boxes describe the analysis performed and green boxes contain the
30 results of the analysis. Arrows indicate for which analyses the datasets were used, the order of the
31 analyses and the results from each analysis.

32 **Figure 2.** Manhattan plot showing the results of the EWAS meta-analysis of *APOE* $\epsilon 4$ vs. $\epsilon 2$ carriers
33 and the positions of DMRs identified in a meta-DMR analysis. Each point represents one of the
34 772,453 loci included in the EWAS meta-analysis, with the point's position being determined by
35 genomic position (x-axis) and significance in the EWAS meta-analysis ($-\log_{10} P$ value; y-axis). Sites
36 attaining genome-wide significance ($P \leq 3.6 \times 10^{-8}$) are indicated in red and those that are involved in
37 a significant DMR (Bonferroni-correct $P \leq 0.05$) are indicated in blue. The locations of DMRs are
38 further indicated by vertical blue lines. The solid horizontal line is the threshold for genome-wide
39 significance ($P \leq 3.6 \times 10^{-8}$) and the dashed line indicates a suggestive significance threshold ($P \leq 1 \times$
40 10^{-5}).

41 **Figure 3.** Circular plot indicating the genomic locations (hg19/GRCh37) of CpGs identified as being
42 DMPs or in DMRs identified in *APOE* $\epsilon 4$ vs. $\epsilon 2$ carriers (blue lines on second track), the meQTLs
43 associated with these CpGs (red lines on third track), and connections between CpGs and meQTLs
44 indicating regulatory relationships (*cis* interactions in red; *trans* interactions in blue). Gene symbols
45 for genes located in each CpG/meQTL-harboring region are indicated.





CEACAM20/IGSF23/PVR/CEACAM19/CEACAM16/BCL3/CBLC/BCAM/PVRL2/TOMM40/APOE/APOC1/APOC4-APOC2/CLPTM1/RELB/CLASRP/ZNF296/GEMIN7/PPP1R37/NKPD1/TRAPPC6A/BLOC1S3/EXOC3L2

EP300/L3MBTL2/CHADL/RANCAP1/ZC3H7B/TEF/TOB2/PHF5A/ACO2/POLR3H/CSDC2/PMM1/DES11/XRCC6/NHP2L1/c22orf46/MEI1/SREBF2/CCDC134/TNFRSF13C/CENPM/SEPT3/WBP2NL/NAGA/FAM109B/SMDT1/NDUFA6/CYP2D6/TCF20

ABCG1

TTC22/LEXM/DHCR24

LDLR

ATP8B4/SLC7A2

SCARB1

CBX5/HNRNPA1/NFE2/COPZ1

GRAMD1B

MYRF/FEN1/TMEM258/FADS1/MIR1908/FADS2

ZNF572/SQLE/KIAA0196/NSMCE2

INSIG1

C6orf183/LOC100996634/CCDC162P

LOC731424/MIR945HG/MIR945

